g factor of the first excited state in ^{56}Fe and implications for transient-field calibration in the Fe region

M. C. East,[1] A. E. Stuchbery,[1] S. K. Chamoli,[1] A. N. Wilson,[1,2] H. L. Crawford,[3] J. S. Pinter,[3] T. Kibédi,[1] and P. F. Mantica[3]

[1]*Department of Nuclear Physics, Research School of Physics and Engineering, The Australian National University Canberra, ACT 0200, Australia*

[2]*Department of Physics, The Australian National University, Canberra, ACT 0200, Australia*

[3]*NSCL and Department of Chemistry, Michigan State University, Michigan 48824, USA*

(Received 22 September 2008; published 5 February 2009; publisher error corrected 14 July 2009)

The transient-field technique has been used to measure the g factor of the 2_1^+ state in ^{56}Fe relative to the independently determined g factor of the first $5/2^-$ state in ^{57}Fe. The new result for ^{56}Fe agrees with previous measurements but is more precise. Implications for calibrating the transient field and g-factor measurements in the fp region are discussed.

DOI: 10.1103/PhysRevC.79.024303 PACS number(s): 21.10.Ky, 27.40.+z, 25.70.De, 23.20.En

I. INTRODUCTION

The transient-field technique in inverse kinematics offers the possibility of measuring the *relative* g factors of excited states in $f_{7/2}$ and fp shell nuclei with a precision of a few percent. Many such measurements have been reported recently. (For reviews, see Refs. [1,2].)

A potential problem arises, however, when it comes to determining the *absolute* g factors. The reference point for transient-field calibrations in this region [3–6] is the g factor of the first-excited state in ^{56}Fe, for which $g = +0.61 \pm 0.08$ has been adopted for the past two decades [7–9]. Unfortunately, as will be shown below, the uncertainty in this value is underestimated: the correct average value based on previously published data should be $g(2_1^+; {}^{56}\mathrm{Fe}) = +0.61 \pm 0.13$, having an experimental uncertainty of $\sim\pm 21\%$.

In the worst-case scenario, the absolute g factors in the $f_{7/2}$ and fp regions determined in transient-field measurements could be uncertain by about $\pm 20\%$. Most of the recent transient-field measurements, however, have been calibrated using one of the "global" parametrizations of the transient-field strength, which might reduce the effect of the uncertainty in the ^{56}Fe g factor. The present paper addresses the problem of transient-field calibration in the Fe region by making a new transient-field measurement on the g factor of the 2_1^+ state in ^{56}Fe, relative to the precisely known g factor of the first $5/2^-$ state at 136 keV in ^{57}Fe, which has been measured by the time-differential perturbed angular distribution (TDPAD) technique [10].

The paper is arranged as follows: Section II reviews the previous measurements of $g(2_1^+)$ in ^{56}Fe. The following two sections describe the experimental techniques and present the experimental results. In Sec. V the implications of the new g-factor measurement are discussed. A summary and conclusions follow.

II. PREVIOUS MEASUREMENTS OF $g(2_1^+)$ IN ^{56}Fe

The value of $g(2_1^+)$ for ^{56}Fe that has been commonly adopted for the past two decades [7–9] is an average of three earlier studies: two by radioactivity techniques [11,12] and one by the "thick-foil" transient-field implantation perturbed angular correlation (IMPAC) technique [13]. In this section, we argue that the latter measurement should be discarded.

The first radioactivity measurement, by Metzger [11], used resonance scattering of γ rays from a ^{56}Co source along with the internal (static) hyperfine field for Fe in iron to measure the perturbations of the $0^+ \to 2^+ \to 0^+$ $\gamma\gamma$ angular correlation. When corrected to reflect the 2^+ level lifetime, $\tau = 9.58 \pm 0.39$ ps, adopted in the recent compilation of Raman *et al.* [14], the resultant gyromagnetic ratio is $g = +0.59 \pm 0.18$.

The second radioactivity measurement, by Appel and Mayer [12], measured perturbed $\gamma\gamma$ angular correlations for the $4^+ \to 2^+ \to 0^+$ transition in ^{56}Fe populated by the decay of ^{56}Co present as a dilute impurity in an iron host. When corrected for new lifetime data [14], their result is $g = +0.64 \pm 0.19$.

The average of these two radioactivity results is $g = +0.61 \pm 0.13$.

As we will now discuss, a close examination of the IMPAC measurement [13] shows that it should not be included in an average with the radioactivity data to obtain an 'adopted' g factor.

In thick-foil transient-field measurements like that performed by Hubler, Kugel, and Murnick [13], the observed precession of the 2^+ state is given by

$$\Delta\theta = g[\phi_{\mathrm{tf}} + \omega\tau\, e^{-t_e/\tau}], \tag{1}$$

where

$$\phi_{\mathrm{tf}} = -\frac{\mu_N}{\hbar}\int_0^{t_s} B_{\mathrm{tf}}(v[t])e^{-t/\tau}dt, \tag{2}$$

and

$$\omega = -\frac{\mu_N}{\hbar}B_{\mathrm{sf}}. \tag{3}$$

In the above equations, g is the nuclear g factor and τ the mean life of the nuclear state. B_{tf} is the transient-field strength, which depends on the ion velocity v, and B_{sf} is the equilibrium static- field strength; t_s is the time at which the ion stops within the ferromagnetic layer (about 1 ps), and t_e is the effective time at which the static hyperfine field reaches its

equilibrium value after the implantation. In early work, it was assumed that $t_e = t_s$; however, it has since been shown that because of the violence of the implantation process, the static field in IMPAC measurements with iron hosts typically takes $t_e \sim 5$ ps to reach its equilibrium strength [15]. The transient field is always positive; however, for Fe in iron, the static field is negative, so the static- and transient-field terms in Eq. (1) tend to cancel.

Hubler *et al.* fitted Eq. (1) to precession data for ^{56}Fe implanted into iron at a range of initial energies up to about 2.5 MeV. They set $B_{\rm sf} = 33$ T and $t_e = t_s$ and varied the g factor along with a parameter that determined the strength of the transient field. The radioactivity data [11,12], which correspond to an implantation energy of zero, and hence $\phi_{\rm tf} = 0$, were included in the fit. The value obtained was $g = +0.60 \pm 0.10$.

Since this IMPAC g-factor result for ^{56}Fe includes the radioactivity data, it is not valid to then combine it (again) in an average with the same radioactivity data, as has been done to obtain the $g(2_1^+)$ value adopted for the past couple of decades [7–9].

Unfortunately, the IMPAC result [13] is only as reliable as the average of the radioactivity measurements it incorporates: In 1974, it was not known that the transient field *increases* with increasing ion velocity. Instead, as generally accepted at the time, Hubler *et al.* assumed that the transient field *decreases* with ion velocity, as predicted by the Lindhard-Winther theory [16]. When Eberhardt and Dybdal [3] reexamined this IMPAC data in 1980, taking into account that the transient field increases with ion velocity, they found it necessary to reduce the static-field strength to $B_{\rm sf} = 22 \pm 2$ T, about 63% of the value used by Hubler *et al.* This observation agrees very well with the subsequent discovery that $t_e \sim 5$ ps is significantly longer than $t_s \sim 1$ ps, since for the 2_1^+ state of ^{56}Fe with $\tau \sim 10$ ps, $e^{-t_e/\tau} \approx e^{-0.5} = 0.61$. [See Eq. (1).] While the IMPAC data can be used to study the velocity dependence of the transient field and possibly to examine radiation effects on the static hyperfine field, neither term inside the square brackets in Eq. (1) is sufficiently well determined to obtain an independent measure of the g factor.

To summarize, of the three previous g-factor measurements on the first excited state in ^{56}Fe, only the two radioactivity measurements can be included in a weighted-average value. The value so obtained, $g = +0.61 \pm 0.13$, has the same numerical value as has been recorded in the data compilations [8,9], but the uncertainty is larger.

III. EXPERIMENTAL METHOD

The g factor of the first 2_1^+ state in ^{56}Fe was measured relative to that of the $5/2_1^-$ state in ^{57}Fe using the transient-field technique with projectile excitation and inverse kinematics [1,2].

The $5/2^-$ state at 136 keV in ^{57}Fe has a mean life of $\tau = 12.6$ ns [17] and $g = +0.374 \pm 0.004$ [10]. Despite its long lifetime, which may suggest small electromagnetic coupling to the lower-lying states, this state can be excited prolifically in Coulomb excitation. It is one of very few cases where TDPAD and transient-field g-factor measurements are both possible. The transient-field precession measurement is difficult, however, because the state decays predominantly (89%) by an almost isotropic 122 keV $5/2^- \rightarrow 3/2^-$ transition to the first excited state at 14 keV. The precession measurement must rely on the weaker (11%) 136 keV $5/2^- \rightarrow 1/2^-$ decay to the ground state. There are also complications due to the long lifetime and the consequent precession of the level in the external field, which will be discussed below.

Beams of ^{56}Fe and ^{57}Fe at 110 MeV were provided by the Australian National University 14UD Pelletron accelerator. The ion-source sample for ^{56}Fe was natural iron powder pressed into a standard copper cathode. For the measurements on ^{57}Fe (abundance 2.2%), which required several runs, both natural and enriched (∼15–20% ^{57}Fe) samples were used. For most samples, oxide beams, FeO^-, exceeded the intensity of Fe^- by an order of magnitude and were injected into the accelerator.

The relatively low beam energy of ∼2 MeV/nucleon was set to ensure that multiple Coulomb excitation of ^{57}Fe beams was kept to a minimum. At this beam energy, multiple excitation of ^{56}Fe is negligible.

The target used for both beams consisted of a 3.4 mg/cm^2 thick gadolinium foil. After rolling and annealing under vacuum, a 0.03 mg/cm^2 layer of copper was evaporated onto the beam-facing side (front) of the target, and a thicker 6 mg/cm^2 layer of copper was evaporated on the back. A 0.6 mg/cm^2 layer of carbon was added to the front of the target by applying a suspension of carbon powder in isopropyl alcohol. Additional tantalum foil (4.5 μm) was placed behind the target to stop the beam. The target was cooled to ∼5 K throughout the experiment by mounting it on the second stage of a cryocooler (Sumitomo RDK-408D). The experimental apparatus is described in more detail elsewhere [19]. Beam intensities, typically ∼0.5 pnA, were kept below 1 pnA.

An external magnetic field must be applied to magnetize the gadolinium layer of the target. The direction of this field is reversed periodically to minimize systematic errors. Our standard procedure for most transient-field measurements is to apply a field of 0.09 T, which is a good compromise between maximizing the magnetization of rolled gadolinium target foils and keeping beam-bending effects negligible. However, the lifetime of the $5/2_1^-$ level in ^{57}Fe, $\tau = 12.6$ ns, is sufficiently long that the precession due to an external field of $B_{\rm ext} = 0.09$ T is $\Delta\theta_{\rm ext} \sim 20$ mrad, comparable to the expected transient-field precession. For the the majority of the experiments reported here, $B_{\rm ext}$ was therefore reduced to 0.01 T, so that $\Delta\theta_{\rm ext} \sim 2$ mrad. An undesirable effect of reducing the external field is that the magnetization of the gadolinium foil, and hence the transient-field effect, is reduced by about 30% (see below).

The deexciting γ rays from the Fe isotopes were measured in coincidence with forward-scattered carbon ions detected by an array of three silicon photodiode detectors 28.9 mm downstream from the target, arranged in a vertical stack as shown in Fig. 1.

To measure the transient-field precessions in ^{57}Fe, two 50% (relative efficiency) high-purity germanium (HPGe) detectors and two 20% HPGe detectors were placed at ±65° and ±115° to the beam axis, respectively. The target-detector

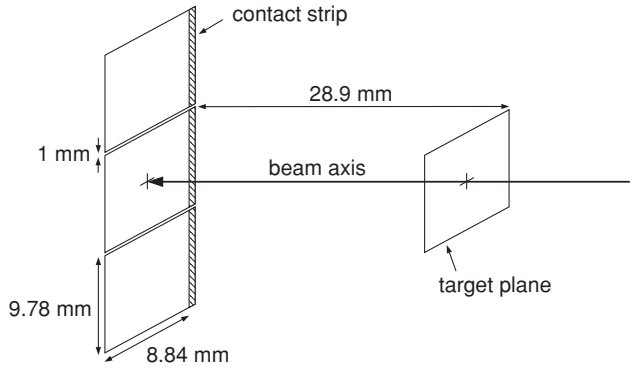

FIG. 1. Schematic view of the arrangement of the particle detectors. The dimensions of the active area are indicated on the lower detector.

distances were set so that the detector crystals all subtended a half angle of 18°. Most of the precession data for ^{56}Fe were taken with the two 20% HPGe detectors (at ±115°) replaced by NaI detectors, as described in Ref. [18].

Precession data for ^{56}Fe were taken for ∼1.5 days of beam time. The corresponding measurement on ^{57}Fe took ∼8 days. A fraction of the ^{57}Fe data (∼12 h) was taken with $B_{\rm ext}$ = 0.09 T to obtain a measure of the external field experienced by the ions stopped in the target backing.

Particle-γ angular correlations were measured for both ^{56}Fe and ^{57}Fe. For ^{56}Fe, where two NaI and two Ge detectors were in use, the detectors in the positive hemisphere were initially kept at +65° and +115°, to provide the normalization, while the other two detectors sampled the angular correlation, sequentially, at five negative angles. The process was then reversed: the detectors in the negative hemisphere remained at −115° and −65°, while the angular correlations were measured at positive angles. Each data point in the angular correlation was measured for ∼2 h.

For the ^{57}Fe angular correlation measurement, the backward-placed Ge detectors were kept at ±115° to normalize the number of counts, while the angular correlation was sampled with the two forward Ge detectors at ±65°, ±60°, ±55°, ±45° and ±30°, in turn. Each data point for the angular correlation was measured for ∼1.5 h, long enough to obtain ∼1000 counts, after background subtraction, in the 136 keV $5/2^-_1 \rightarrow 1/2^-_1$ transition in ^{57}Fe.

IV. RESULTS AND ANALYSIS

A. Experimental results

Precession angles due to the transient field were obtained by standard procedures [1,2]. The g factor is proportional to the experimental precession angle, which is given by $\Delta\Theta = \epsilon/S$, where S is the logarithmic derivative of the angular correlation at the γ-ray detection angle. The "effect" ϵ was evaluated from double ratios of counts recorded for field up and field down in the pairs of detectors at ±65° and ±115° [20]. Formally, $\epsilon = (N\downarrow - N\uparrow)/(N\downarrow + N\uparrow)$, where N is the number of counts detected at angle θ, and ↑ and ↓ denote the direction of the magnetic field.

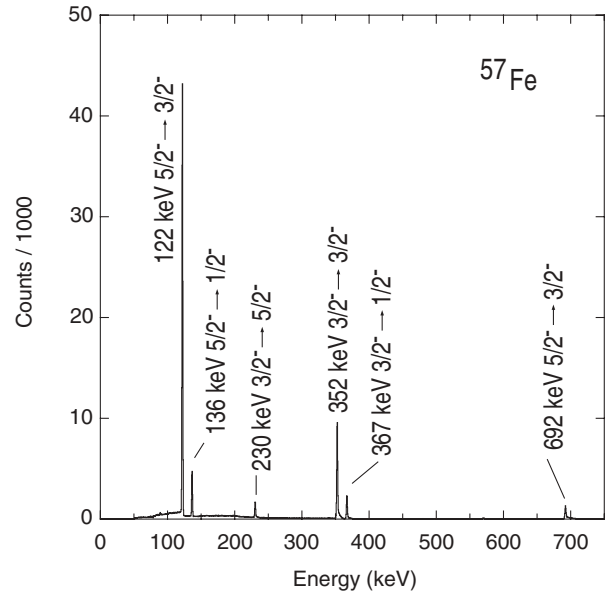

FIG. 2. Spectrum of ^{57}Fe γ rays observed at +65° to the beam axis in coincidence with the central particle detector. This spectrum represents about 16 h of data for the field-up direction, obtained during the precession measurement.

To determine ϵ, γ-ray spectra in coincidence with carbon ions were produced for each direction of the magnetic field. After random subtraction, there were no observable contaminants, and no excitation to states above the 2^+_1 state was observed in ^{56}Fe. Figure 2 shows an example of a random-subtracted γ-ray spectrum for ^{57}Fe. Along with the excitation of the 136 keV $5/2^-$ state, there is much weaker excitation of higher excited states at 367 keV ($3/2^-_2$) and 706 keV ($5/2^-_2$). Of the lines above 136 keV in Fig. 2, only the 230 keV, $3/2^-_2 \rightarrow 5/2^-_1$ transition feeds into the 136 keV $5/2^-_1$ level. The effect of this feeding contribution on the angular correlation and g-factor measurements is therefore extremely small. No evidence for multiple excitation was observed in ^{56}Fe (see Ref. [18] for a representative γ-ray spectrum).

Data were analyzed for the three particle detectors separately. Because of the symmetry, the experimental observables are the same for the upper and lower (outer) particle detectors. Table I outlines the reaction kinematics and level mean lives for the two Fe isotopes of interest. The reaction kinematics and energy loss differ for the central versus outer detectors. For the present case, this difference in kinematic conditions is of minor consequence, as is evident from the uniformity of the calculated transient-field precessions per unit g factor, $\phi_{\rm calc}$, shown in the final column of Table I. [$\phi_{\rm calc}$ is the calculated value of $\phi_{\rm tf}$ defined in Eq. (2).] These calculations were performed assuming that the transient field follows a linear dependence on ion velocity. The rationale for this choice of transient-field parametrization, and further details of the calculational procedure, are given in Ref. [18].

Angular correlations were calculated based on the theory of Coulomb excitation [21]. These calculations took into account the energy loss of the beam in the target and averaged the statistical tensors over the solid angle of the particle detectors. Further details of the calculation procedures have been given in

TABLE I. Reaction kinematics and nuclear properties. $\tau(2_1^+)$ is the mean life. $\langle E_i \rangle$ and $\langle E_e \rangle$ are the energies at which Fe ions enter and leave the ferromagnet; $\langle v_i/v_0 \rangle$ and $\langle v_e/v_0 \rangle$ are the corresponding velocities (Bohr velocity $v_0 = c/137$). $\langle v/v_0 \rangle$ is the average velocity for the Fe nucleus in the ferromagnet, and $t_{\rm Gd}$ is the effective time spent in the ferromagnet. $\phi_{\rm calc}$ is defined in Eq. (2) and evaluated for $B_{\rm tr} = 14Zv/v_0$ T. Further details of the calculations are given in Ref. [18].

Isotope	$\tau(2_1^+)$[a]	Particle detector	$\langle E_i \rangle$ (MeV)	$\langle E_e \rangle$ (MeV)	$\langle v_i/v_0 \rangle$	$\langle v_e/v_0 \rangle$	$\langle v/v_0 \rangle$	$t_{\rm Gd}$ (fs)	$\phi_{\rm calc}$ (mrad)
^{56}Fe	9.6 ps	Center	30.7	4.9	4.70	1.87	3.05	623	32.94
		Outer	36.9	7.2	5.16	2.27	3.52	550	33.46
^{57}Fe	12.6 ns	Center	31.4	5.2	4.71	1.92	3.08	645	34.39
		Outer	37.4	7.5	5.14	2.31	3.52	571	34.78

[a]Mean lives from Refs. [14,17].

Refs. [20,22,23]; however, here the calculations were modified for inverse kinematics. For the mixed-multipolarity 122 keV $5/2^- \rightarrow 3/2^-$ transition in ^{57}Fe, the mixing ratio was taken from Ref. [17].

Because the electromagnetic interaction conserves parity, the angular correlation for ions detected in the top particle detector is identical to that for ions detected in the bottom particle detector. The data for the outer (i.e., top and bottom) particle detectors are therefore added together for presentation here.

Figure 3 shows the measured and calculated angular correlations for the $2_1^+ \rightarrow 0^+$ 847 keV transition in ^{56}Fe as observed in coincidence with the center and outer particle detectors. Figure 4 shows the corresponding angular correlations for the $5/2_1^- \rightarrow 1/2_1^-$ 136 keV and $5/2_1^- \rightarrow 3/2_1^-$ 122 keV transitions in ^{57}Fe. The only free parameters in these fits were a normalization factor and a possible angular offset, in case the axis of the detector crystal was not perfectly aligned to the angle read on the correlation table. This offset, which can vary from detector to detector, is frequently consistent with zero, and generally less than 3°.

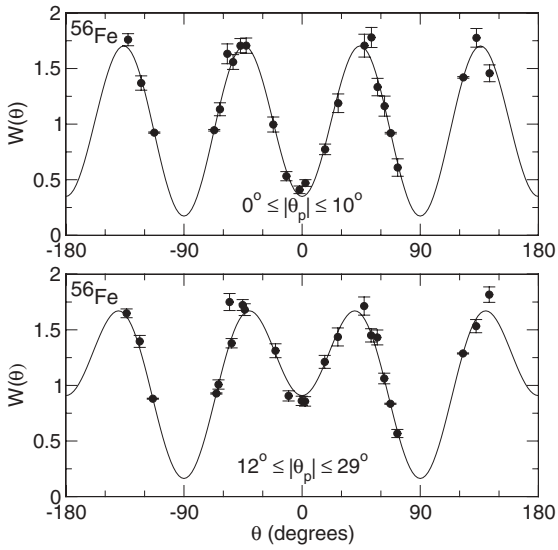

FIG. 3. Measured and calculated (unperturbed) angular correlations for ^{56}Fe in inverse kinematics. The upper panel is for the center particle detector, the lower panel is for the top and bottom (outer) detectors. The range of particle detection angles in the vertical plane, above and below the beam axis, is indicated.

In the present case, the solid angle attenuation coefficients for all four detectors are almost identical, well within the precision of both the angular correlation and precession measurements. The comparisons of theory and experiment in Figs. 3 and 4 therefore combine the data for all γ-ray detectors for which the correlations were measured.

Events recorded at the center of the central particle detector correspond to head-on collisions. The observed angular correlations for the central detector are therefore close to the case in which the nuclear spin is aligned in the plane perpendicular to the beam. For the outer detectors, the correlation is no longer head-on in the center of mass. As seen in Figs. 3 and 4, the main change in the angular correlation is near $\theta_\gamma = 0°$ (and 180° for the $2^+ \rightarrow 0^+$ transition). The differences are more subtle for the decays in ^{57}Fe than for the $2^+ \rightarrow 0^+$ transition in ^{56}Fe. In all cases, there is only a small change in the angular correlation (and its slope) for $|\theta_\gamma|$ between 45° and 135°, i.e., where the detectors are placed for the precession measurements.

The excellent agreement between the measured and calculated angular correlations for both ^{56}Fe and ^{57}Fe is in accord with the extensive comparisons between experimental

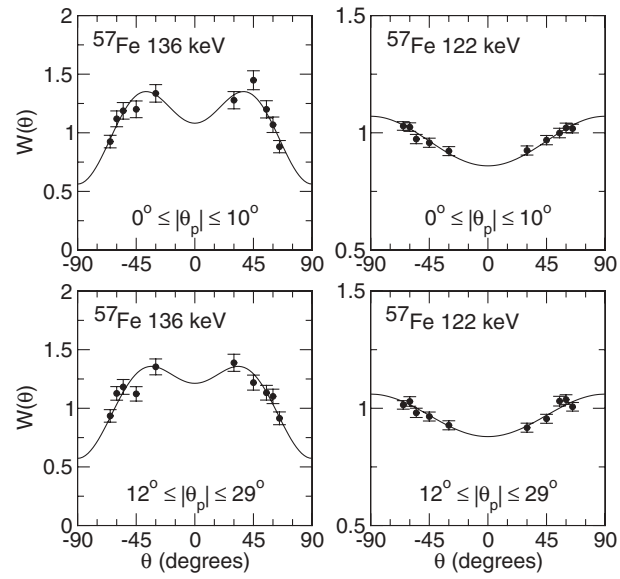

FIG. 4. Similar to Fig. 3, but showing the measured and calculated angular correlations for the $5/2_1^- \rightarrow 1/2_1^-$ 136 keV (left panels) and $5/2_1^- \rightarrow 3/2_1^-$ 122 keV (right panels) transitions in ^{57}Fe.

and theoretical angular correlations after Coulomb excitation previously reported by our group. (See, for example, Refs. [24–27]; a more comprehensive list of references is given in Ref. [20].) For the analysis of the precession data, the calculated angular correlations are used. In the present case, the uncertainties in the calculated S values are negligible compared with the statistical uncertainties in the measured effects ϵ.

B. External field correction

As noted above, the external field contributes significantly to the total precession observed for the $5/2_1^-$ level in ^{57}Fe. Thus, using an obvious notation, we write

$$\Delta\theta_{\rm obs} = \Delta\theta_{\rm tf} + \Delta\theta_{\rm ext}. \tag{4}$$

Dividing through by the known g factor, and using the notation $\phi = \Delta\theta/g$, gives

$$\phi_{\rm obs} = \phi_{\rm tf} + \phi_{\rm ext}. \tag{5}$$

Clearly, $\phi_{\rm ext} = -(\mu_N/\hbar)B_{\rm ext}\tau$ is proportional to the effective external field experienced by the Fe ions in the target backing. As a first approximation, $B_{\rm ext}$ can be set equal to the applied field measured in the target position with the target removed. Some caution is needed, however, because the ferromagnetic layer of the target will tend to concentrate the flux through that region of the target and may change the effective field in the adjacent copper backing layer where the Fe ions stop. A series of schematic calculations were run with Superfish software [28] to calculate the difference between the effective field in the target backing and the field measured in the target location with the target removed. It was concluded that the ferromagnetic layer of the target is sufficiently thin that these fields can be assumed equal within a few percent.

In an effort to get an experimental verification of this conclusion, the total precession angles were measured for both ^{56}Fe and ^{57}Fe with the polarizing field set to 0.01 T (LF = low field) and 0.09 T (HF = high field). The results are given in Table II. For ^{56}Fe, $\phi_{\rm ext}$ is negligible; the resultant value of $\phi_{\rm tf}^{\rm LF}/\phi_{\rm tf}^{\rm HF} = 0.69(4)$ shows that the magnetization achieved for the Gd layer of the target is smaller with the lower applied field by about 30%. (Similar effects have been found for rolled and annealed iron foils [29].)

Under the assumption that the ratio of effective fields at the Fe nuclei in the target backing scales as the ratio of the applied fields measured with the target removed, we have two equations for the ^{57}Fe precessions that can be solved to give $B_{\rm ext}^{\rm LF}$ and $B_{\rm ext}^{\rm HF}$, namely,

$$\phi_{\rm obs}^{\rm LF} = (0.69 \pm 0.04)\phi_{\rm tf}^{\rm HF} + \phi_{\rm ext}^{\rm HF}/9, \tag{6}$$

and

$$\phi_{\rm obs}^{\rm HF} = \phi_{\rm tf}^{\rm HF} + \phi_{\rm ext}^{\rm HF}. \tag{7}$$

The result is $B_{\rm ext}^{\rm LF} = 0.012(4)$ T and $B_{\rm ext}^{\rm HF} = 0.111(35)$ T, consistent with the applied fields measured in the target position with the target removed.

To correct for the external field precession, we therefore take the effective field at the ^{57}Fe nuclei in the target backing to be equal to that measured in the target position with the target removed. An uncertainty of $\pm 20\%$ is assigned to this value, sufficient to cover uncertainties in the measurement of the field in the target position and any change in its value due to the ferromagnetic layer of the target.

A summary of the precession results, including corrections for kinematic differences, finite lifetimes, and the external field precession of the $5/2^-$ state in ^{57}Fe, is given in Table II. Ratios of $\Delta\theta$ values in the final column of this table correspond to g-factor ratios.

V. DISCUSSION

The present and previous g-factor measurements on the 2_1^+ state in ^{56}Fe are summarized in Table III. The adopted weighted average value is dominated by the present measurement with the "low" external field. The new result is consistent with the previously adopted value within the experimental uncertainties but is more precise. The experimental g factor for the first excited state in ^{56}Fe is now closer to the collective estimate, $g = Z/A \simeq 0.46$, than suggested by the previous data.

There are implications of the present result for the calibration of the transient field in the region of $Z = 26$. It is not the purpose here to attempt a new parametrization of the transient-field strength in terms of the ion velocity and atomic number. Rather, discussion will be confined to implications

TABLE II. Summary of measured precession angles.[a]

Isotope	E_γ (keV)	$B_{\rm ext}$ (T)	$\langle\Delta\theta\rangle_{\rm outer}$ (mrad)	$\langle\Delta\theta\rangle_{\rm center}$ (mrad)	$\langle\Delta\theta\rangle_{\rm obs}$ (mrad)	$\Delta\theta_{\rm ext}$ (mrad)	$\Delta\theta$ (mrad)
^{56}Fe	847	0.01	−14.8(9)	−15.1(11)	−14.89(70)	0.0	−14.89(70)
^{57}Fe	122	0.01	−16.6(46)	−10.2(53)	−13.8(34)[b]		
	136	0.01	−13.3(17)	−13.4(19)	−13.4(13)[b]		
				^{57}Fe average:	⟨−13.41(118)⟩[b]	−2.37(48)	−11.04(127)
^{56}Fe	847	0.09	−22.0(12)	−21.1(13)	−21.55(86)	0.0	−21.55(86)
^{57}Fe	122	0.09	−48(23)	−43(27)	−46(18)[b]		
	136	0.09	−34(9)	−47(10)	−39.7(67)[b]		
				^{57}Fe average:	⟨−40.5(62)⟩[b]	−20.3(4.1)	−20.2(75)

[a]Slopes of the angular correlations at +65° (in rad^{-1}) are for ^{56}Fe: $S_{\rm center} = -2.65$ and $S_{\rm outer} = -2.71$; for ^{57}Fe 122 keV: $S_{\rm center} = 0.15$ and $S_{\rm outer} = 0.15$; for ^{57}Fe 136 keV: $S_{\rm center} = -1.43$ and $S_{\rm outer} = -1.37$.
[b]These precession values include a contribution from the external field.

TABLE III. Summary of g-factor measurements in ^{56}Fe.

Measurement	$g(2_1^+)$
Present low field	+0.504(63)
Present high field	+0.40(15)
Radioactivity [11,12]	+0.61(13)
Average	+0.509(53)

of our measurement for transient-field measurements in the $f_{7/2}$ and fp shells, many of which have been performed by the Bonn group (see, for example, Refs. [1,5,6] and references therein).

The approach used by the Bonn group is to begin with the linear parametrization of the transient-field strength as originally proposed by Eberhardt *et al.* [30], that is,

$$B_{\rm tf} = a_{\rm lin} Z v/v_0, \tag{8}$$

where $a_{\rm lin} = 17(1)$ T for Gd hosts [31]. For heavier beams, it is necessary to modify this parametrization. The procedure adopted by the Bonn group is to replace $a_{\rm lin}$ by the product $a_{\rm lin} G_{\rm beam}$, where $G_{\rm beam}$ is an attenuation factor that depends on the energy deposited by the beam in the target. For their measurement on ^{54}Fe, Speidel *et al.* [1,5] used $G_{\rm beam} = 0.83(3)$, so that, in effect, $a_{\rm lin} = 14.1(7)$ T in Eq. (8). In Ref. [5], transient-field precessions were measured to check the adopted value of $G_{\rm beam}$. If the data for ^{56}Fe in Table I of Ref. [5] are interpreted as a g-factor measurement based on the adopted parametrization, the result is $g = 0.55(3)$, where the error is dominated by the uncertainty assigned to the field calibration.[1] On one hand, this value is consistent with the independent measurements on ^{56}Fe in Table III, the average of which is $g = 0.51(5)$. On the other hand, the new data could also be taken to imply that the reported g factors should be reduced by a factor of $\sim$0.9 and assigned an uncertainty of the order of $\pm 10\%$. While the uncertainty on the experimental g factor of ^{56}Fe remains near 10%, both views are tenable. We suggest, however, that caution is warranted when assigning uncertainties to absolute g factors in the $f_{7/2}$ and fp shells measured by the transient-field technique.

[1]The last two entries of the last column of Table I in Ref. [5] report $\Phi^{\rm lin}$ for ^{56}Fe, assuming $g = 0.61(8)$, not $\Phi^{\rm lin}/g$ (K.-H. Speidel, private communication). There is a difference in terminology: Φ in Ref. [5] is the same as $\Delta\theta$ here.

VI. SUMMARY AND CONCLUDING REMARKS

The precision with which the absolute value of the gyromagnetic ratio is known for the 2_1^+ state in ^{56}Fe has been improved significantly by measuring it relative to the independently determined g factor of the $3/2_1^-$ state in ^{57}Fe. The $5/2_1^-$ $\tau = 12.6$ ns state in ^{57}Fe is one of very few cases where TDPAD and transient-field measurements can both be performed. The new result for the g factor in ^{56}Fe is somewhat smaller in magnitude than the previously adopted value, but they agree within the statistical errors.

The present result is important because very few independently determined g factors of excited states in nuclei with atomic numbers between about $Z = 14$ and $Z = 40$ can be used to calibrate the transient field. It would certainly be worthwhile to attempt further improvement in the precision of the measurement of $g(2_1^+)$ in ^{56}Fe, which is currently about $\pm 10\%$. Apart from extending beam time (already about 8 days), it may be possible to improve the precision of the present technique by increasing the beam energy and/or intensity; however, these increases could also have adverse effects (such as increased multiple excitation or damage to the target due to beam heating). Other avenues, such as a new measurement by the integral perturbed angular correlations (IPAC) radioactivity technique [12], should also be considered.

ACKNOWLEDGMENTS

The authors are grateful to the academic and technical staff of the Department of Nuclear Physics (Australian National University) for their assistance. This work was supported in part by the Australian Research Council Discovery Scheme Grant No. DP0773273 and National Science Foundation Grant No. PHY-06-06007. M.C.E. is supported by an Australian Postgraduate Research Award (APRA).

[1] K.-H. Speidel, O. Kenn, and F. Nowacki, Prog. Part. Nucl. Phys. **49**, 91 (2002).
[2] N. Benczer-Koller and G. J. Kumbartzki, J. Phys. G: Nucl. Part. Phys. **34**, R321 (2007).
[3] J. L. Eberhardt and K. Dybdal, Hyperfine Interact. **7**, 387 (1980).
[4] N. K. B. Shu, D. Melnik, J. M. Brennan, W. Semmler, and N. Benczer-Koller, Phys. Rev. C **21**, 1828 (1980).
[5] R. Ernst, K. H. Speidel, O. Kenn, A. Gohla, U. Nachum, J. Gerber, P. Maier-Komor, N. Benczer-Koller, G. J. Kumbartzki, G. Jakob *et al.*, Phys. Rev. C **62**, 024305 (2000).
[6] K.-H. Speidel, R. Ernst, O. Kenn, J. Gerber, P. Maier-Komor, N. Benczer-Koller, G. J. Kumbartzki, L. Zamick, M. S. Fayache, and Y. Y. Sharon, Phys. Rev. C **62**, 031301(R) (2000).
[7] J. M. Brennan, N. Benczer-Koller, M. Hass, and H. T. King, Phys. Rev. C **16**, 899 (1977).
[8] P. Raghavan, At. Data Nucl. Data Tables **42**, 189 (1989).
[9] N. J. Stone, At. Data Nucl. Data Tables **90**, 75 (2005).
[10] C. Fahlander, K. Johansson, and G. Possnert, Phys. Scr. **20**, 163 (1979).
[11] F. R. Metzger, Nucl. Phys. **27**, 612 (1961).
[12] H. Appel and W. Mayer, Nucl. Phys. **43**, 393 (1963).
[13] G. K. Hubler, H. W. Kugel, and D. E. Murnick, Phys. Rev. C **9**, 1954 (1974).
[14] S. Raman, C. W. Nestor, and P. Tikkanen, At. Data Nucl. Data Tables **78**, 1 (2001).

[15] A. E. Stuchbery and E. Bezakova, Phys. Rev. Lett. **82**, 3637 (1999).
[16] J. Lindhard and A. Winther, Nucl. Phys. **A166**, 413 (1971).
[17] M. R. Bhat, Nucl. Data Sheets **85**, 415 (1998).
[18] M. C. East, A. E. Stuchbery, S. K. Chamoli, A. N. Wilson, H. L. Crawford, J. S. Pinter, T. Kibédi, and P. F. Mantica, Phys. Rev. C **79**, 024304 (2009).
[19] A. E. Stuchbery, A. B. Harding, D. C. Weisser, N. R. Lobanov, and M. C. East (in preparation).
[20] A. E. Stuchbery, A. Nakamura, A. N. Wilson, P. M. Davidson, H. Watanabe, and A. I. Levon, Phys. Rev. C **76**, 034306 (2007).
[21] A. Winther and J. de Boer, in *Coulomb Excitation*, edited by K. Alder and A. Winther (Academic Press, New York, 1966), p. 303.
[22] A. E. Stuchbery, Australian National University, Rep. No. ANU-P/1678, 2005, arXiv:nucl-ex/0609032.
[23] A. E. Stuchbery, A. N. Wilson, P. M. Davidson, and N. Benczer-Koller, Nucl. Instrum. Methods Phys. Res. B **252**, 230 (2006).
[24] A. E. Stuchbery, I. Morrison, L. D. Wood, R. A. Bark, H. Yamada, and H. H. Bolotin, Nucl. Phys. **A435**, 635 (1985).
[25] A. E. Stuchbery, G. J. Lampard, and H. H. Bolotin, Nucl. Phys. **A528**, 447 (1991).
[26] S. S. Anderssen, A. E. Stuchbery, and S. Kuyucak, Nucl. Phys. **A593**, 212 (1995).
[27] P. F. Mantica, A. E. Stuchbery, D. E. Groh, J. I. Prisciandaro, and M. P. Robinson, Phys. Rev. C **63**, 034312 (2001).
[28] Poisson Superfish, Los Alamos Accelerator Code Group, http://laacg.lanl.gov/laacg.
[29] A. E. Stuchbery and E. Bezakova, Aust. J. Phys. **51**, 183 (1998).
[30] J. L. Eberhardt, R. E. Horstman, P. C. Zalm, H. A. Doubt, and G. van Middelkoop, Hyperfine Interact. **3**, 195 (1977).
[31] K.-H. Speidel, U. Reuter, J. Cub, W. Karle, F. Passek, H. Busch, S. Kremeyer, and J. Gerber, Z. Phys. D **22**, 371 (1991).